PHILOSOPHICAL TRANSACTIONS OF THE ROYAL SOCIETY B BIOLOGICAL SCIENCES

Flow visualization and unsteady aerodynamics in the flight of the hawkmoth, *Manduca sexta*

Alexander P. Willmott, Charles P. Ellington and Adrian L. R. Thomas

Phil. Trans. R. Soc. Lond. B 1997 **352**, 303-316
doi: 10.1098/rstb.1997.0022

Flow visualization and unsteady aerodynamics in the flight of the hawkmoth, *Manduca sexta*

ALEXANDER P. WILLMOTT*, CHARLES P. ELLINGTON AND ADRIAN L. R. THOMAS†

Department of Zoology, University of Cambridge, Downing Street, Cambridge CB2 3EJ, UK

SUMMARY

The aerodynamic mechanisms employed during the flight of the hawkmoth, *Manduca sexta*, have been investigated through smoke visualization studies with tethered moths. Details of the flow around the wings and of the overall wake structure were recorded as stereophotographs and high-speed video sequences. The changes in flow which accompanied increases in flight speed from 0.4 to 5.7 m s^{-1} were analysed. The wake consists of an alternating series of horizontal and vertical vortex rings which are generated by successive down- and upstrokes, respectively. The downstroke produces significantly more lift than the upstroke due to a leading-edge vortex which is stabilized by a radial flow moving out towards the wingtip. The leading-edge vortex grew in size with increasing forward flight velocity. Such a phenomenon is proposed as a likely mechanism for lift enhancement in many insect groups. During supination, vorticity is shed from the leading edge as postulated in the 'flex' mechanism. This vorticity would enhance upstroke lift if it was recaptured during subsequent translation, but it is not. Instead the vorticity is left behind and the upstroke circulation builds up slowly. A small jet provides additional thrust as the trailing edges approach at the end of the upstroke. The stereophotographs also suggest that the bound circulation may not be reversed between half strokes at the fastest flight speeds.

1. INTRODUCTION

The inadequacy of conventional aerodynamic mechanisms in accounting for the observed lift production during flapping insect flight is now widely accepted by biomechanicists. Early models in which the instantaneous forces were assumed to be identical to those generated by a fixed wing at the same angle of attack and velocity suggested that these 'steady' aerodynamic mechanisms might be sufficient to explain flight in most insect species (e.g. Jensen 1956; Weis-Fogh 1972, 1973). The validity of this 'quasi-steady assumption' has been challenged more recently, however, for a range of species both by detailed quasi-steady analyses of the aerodynamic forces (Ellington 1984*c*; Ennos 1989; Dudley & Ellington 1990; Wakeling 1995; Willmott 1995) and by direct measurements of the instantaneous forces generated by tethered insects (Cloupeau *et al*. 1979; Wilkin 1990; Zanker & Götz 1990; Wilkin & Williams 1993). The focus of research has therefore switched, as suggested by Spedding (1992, 1993), away from debating the need to invoke novel high-lift mechanisms to considering the nature of these mechanisms and how large their contribution is in different flight modes.

As the importance of unsteady aerodynamics for insect flight became apparent, so an increasing number of potential mechanisms were proposed by which lift generation might be enhanced during translational or rotational phases of the wingbeat (e.g. Weis-Fogh 1973; Nachtigall 1979; Ellington 1980, 1984*b*). These mechanisms and the results of subsequent attempts to validate them through numerical analysis or empirical modelling have been reviewed by Ellington (1995).

One feature which appears regularly in these studies is a leading-edge vortex: a separation 'bubble' lying on the upper surface between a flow separation point at the leading edge and a more posterior reattachment point (e.g. Maxworthy 1979; Dickinson & Götz 1993; Sunada *et al*. 1993). The leading-edge vortex effectively increases the camber of the wing, causing an increase in the air velocity over the upper surface of the wing. The resulting increase in the pressure differential across the wing is manifested in enhanced lift generation.

The leading-edge vorticity could, theoretically, be generated by a rotational mechanism such as the 'clap and fling' proposed by Weis-Fogh (1973) for the chalcid wasp, *Encarsia formosa*, or the related 'peel' or 'near peel' which is more typical for larger insects (Ellington 1984*a*). It could, alternatively, be generated by the only significant translatory candidate for unsteady lift enhancement—delayed or dynamic stall (e.g. Kramer 1932; Francis & Cohen 1933). In the latter case, vortex formation will be facilitated both by

* Current addresses: Kawachi Millibioflight Project, Japan Science and Technology Corporation (JST), Park Building 3F, 4-7-6 Komaba, Meguro-ku, Tokyo 153, Japan.
† Department of Zoology, Oxford University, South Parks Road, Oxford, OX1 3PS, UK.

the relatively low Reynolds numbers at which insects fly and by the typically sharp leading edges of their wings (Ellington 1984*b*).

The presence of a leading-edge vortex could potentially have a very pronounced influence on wing performance. Gursul & Ho (1992) found that under optimal conditions the instantaneous lift coefficient for a two-dimensional airfoil undergoing dynamic stall at a Reynolds number of 5×10^4 reached values which were an order of magnitude higher than the maximum steady-state level. Even at the much lower Reynolds number of 192, appropriate to *Drosophila* flight, Dickinson & Götz (1993) observed that a large leading-edge vortex developed during the first two chord lengths of travel of an impulsively started wing at moderate to high angles of attack. This vorticity was accompanied by lift coefficients of about two. The rapidity of the increase in the size of the vortex, however, resulted in its being shed with consequent loss of the lift enhancement after four chords of travel. This situation might not be reached during hovering flight in many insects—the *Manduca* wing, for example, travels 2.5–3 chords at half-wing length (Willmott 1995)—but unless the vortex can be stabilized over the longer half-stroke paths found in forward flight, the benefits of this mechanism will decrease with forward speed.

One possible solution to this problem lies in the qualitative differences in flow between two-dimensional and three-dimensional fling motions noted by Maxworthy (1979). In the latter case there was a strong axial flow within the leading-edge vortex which convected vorticity out towards the wingtip, and into the tip vortex. This spanwise flow may prevent the vortex from becoming too large, thus stabilizing it in a manner similar to well-characterized mechanisms for controlling detached vortices on fixed airfoils (e.g. Campbell 1976; Wu *et al*. 1991).

With regard to other possible mechanisms of lift enhancement during stroke reversal, Dickinson (1994) found that the highest forces were obtained when a flat plate rotated about an axis close to its trailing edge. During the rotation, vorticity is shed at the leading edge which is of the correct sense to add to the bound circulation on the subsequent translation, providing that it can be recaptured. Morphologically, the rotation axis of most insect wings runs close to their leading edge, but rotation about the trailing edge and hence leading-edge shedding could theoretically be encouraged either through an appropriate combination of rotation and wing flexion (e.g. the 'flex' mechanism suggested by Ellington (1984*b*)) or by delaying the rotation relative to the subsequent translation (Ellington 1984*a*).

Experimental and numerical modelling have, therefore, demonstrated the potential of many of the unsteady, high-lift mechanisms, but cannot confirm which of them are actually being used during the much more complicated motions which characterize the flight of real insects. A complementary line of research has focused on flow visualization studies of the vortex wake structure generated by flying insects. The vortices in the wake reflect the pattern of lift and thrust generation, but they do not directly identify the manner in which the enhanced circulation has been generated. The latter requires investigation of the airflow immediately around the wings. The precise timing and location of vortex formation, which can only occur through interaction between the wing and the air, provide the evidence for which mechanism is being employed.

A range of techniques has been employed both for visualizing the flow and for recording the resulting wake structures. Particle visualization facilitates a quantitative analysis of the velocity field, and it has been used for a range of functionally two- and four-winged insects (Ellington 1980; Brodsky & Grodnitsky 1985; Grodnitsky & Morozov 1992, 1993). Smoke streaklines often provide a clearer picture of the details of the flow, especially for the near field, as has been shown by Brodsky (1991). The flows are commonly lit using planar illumination, which produces two-dimensional slices of the wake that are readily analysable (e.g. Brodsky 1991; Grodnitsky & Morozov 1992, 1993). Three-dimensional reconstruction from a series of such slices is possible, but the flow components which are perpendicular to the plane of illumination are difficult to detect. Illumination of the entire wake provides a three-dimensional picture suitable for stereophotographic analysis (e.g. Spedding *et al*. (1984) for slow flight in the pigeon). The high-resolution images obtained by still photography have increasingly been complemented by high-speed cinematography, which can provide useful information on the timing of vortex formation and on the dynamics of the vortex wake (Luttges 1989; Brodsky 1991; Grodnitsky & Morozov 1993).

No unequivocal picture has yet emerged, however, of either the gross wake structure or, more importantly, of the details of the near field flow for any insect group. This paper presents the results of a detailed investigation of the unsteady aerodynamics associated with the flight of the hawkmoth, *Manduca sexta*. The wake behind tethered moths was visualized with smoke trails, and the three-dimensional structure was recorded using both stereophotography and high-speed videography. The influence of flight speed on the wake structure was studied for a range of forward velocities similar to that observed during an analysis of free flight kinematics (Willmott 1995). A complementary study in which a model, robotic hawkmoth was used to undertake further quantitative investigations of the flow forms two companion papers (Van den Berg & Ellington 1997*a*, *b*).

2. MATERIALS AND METHODS

(*a*) *Moths and their tethering*

Adult moths were obtained from a colony maintained by the Department of Zoology, University of Cambridge, UK. Wing deterioration in flight chambers is fairly rapid, and only individuals with undamaged, well-scaled wings were used. In order to control the flight speed and the location of the smoke relative to the insect it was necessary to tether the moths. The tether was designed to permit flight to be as natural as possible. Lift production was monitored

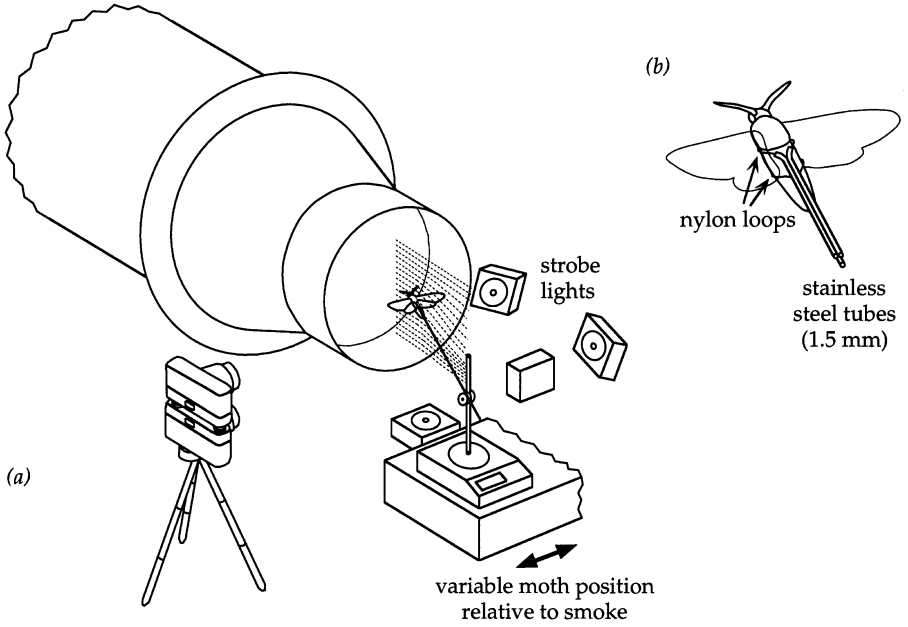

Figure 1. The experimental set-up for stereophotography. (*a*) The camera and strobe light positions relative to the wind tunnel and moth. The frame around the cameras is not shown. (*b*) Details of the tethering system. See text for more details.

so that only flight sequences which corresponded closely to free-flight conditions would be analysed; the moth had to generate a vertical force of at least 70% of its body weight, with no rolling or yawing motion. The moths were chilled at 5 °C for 5 min before use to facilitate tethering.

The moths were tethered 5 cm downstream from the 26 cm diameter, circular opening of an open jet wind tunnel (figure 1*a*). The tether was stiff, consisting of three 1.5 mm diameter stainless steel tubes glued to give an inverted triangular cross-section (figure 1*b*). The moth was attached below the tether by two loops of nylon thread (0.5 mm diameter). The anterior loop, protruding from the ends of the upper two tubes, circled the waist between the thorax and abdomen; the ends of the two tubes diverged slightly to prevent constriction of the dorsal aorta, which is important in thermoregulation during flight (Heinrich 1970, 1971). The posterior loop, threaded through the third tube, was placed loosely around the fourth or fifth abdominal segment to restrict yawing movement. The tether angle, which was adjustable, determined the minimum body angle of the moth; the nature of the tether enabled the animal to increase its body angle by as much as 30 ° above this minimum. The other end of the tether was mounted on a vertical column which replaced the pan of a Mettler BB240 electronic balance. Prior to each experiment, the balance was tared with the moth not yet flying; subsequent readings gave an estimate of vertical force generation.

(*b*) *Experimental set-up for wake visualization and recording*

A vertical, streamlined smoke rake was located on the centre line of the wind tunnel at the upstream end of the contraction area. The 'smoke' was a suspension of oil droplets produced by a System E Integrated Smoke Generator (Nutem Ltd, Crawley, UK), and it was released into the airstream through 52 nylon tubes at 5 mm spacing.

Two Nikon F3 cameras with 50 mm, *f* 1.2 lenses were mounted directly above one another within a metal frame positioned 30 cm from the moths. Their optical axes were perpendicular to the path of the smoke streams but the axes were offset by 10° from each other to allow comfortable viewing of the stereo pairs. Nikon MD-4 motor-drives and bulk film cassettes allowed approximately 250 stereo pairs to be taken before reloading was necessary. Ilford HP5 Plus black and white print film, processed with Microphen developer at 1600 ASA, was used. The cameras were set at an aperture of *f* 2.8 and a shutter speed of 1/30 s throughout the study.

Illumination was provided by four strobe lamps which were positioned to provide maximum contrast between the smoke and a black background. Three were used to back-light the smoke (figure 1*a*), while the fourth was placed directly below the moth to remove the shadows cast by the body and wings. The strobes were synchronized to a Drelloscop 2009 strobe, which was set to a slightly lower rate than the wingbeat frequency, slowing down the apparent wingbeat cycle. The Drelloscop frequency was divided by ten before being passed to the two cameras, where it triggered frame exposure and advance.

The Mettler balance was mounted on the moveable arm of a large photographic stand (John Hadland), which enabled the position of the moth relative to the smoke to be varied both between and during flights.

(*c*) *Experimental procedure*

In the first set of experiments the smoke was located at a spanwise position of 0.5*R*, indicating that when the wing was horizontal it was struck by the trails at a spanwise position halfway between the wingbase and the wingtip. *R* is the wing length. At other instants in the wingbeat cycle, as the wing moved away from this orientation, the point of intersection moved towards the wingtip. The airspeed was varied from 0.4 to 5.7 m s^{-1} in order to assess the effects of flight speed on the wake structure. At each speed, the tether angle was set to the body angle observed during high-speed video filming of *Manduca* in free flight (Willmott 1995).

Further information concerning the three-dimensional structure of the wake was obtained by varying the spanwise position of the smoke. Four locations were used: 0.25, 0.5, 0.75 and 1.0*R*, the latter being at the wingtip. The airspeed was 1.8 m s^{-1} throughout.

Approximately 40–50 frames were taken at each combination of wind speed and smoke position. Between sequences the moth was rested by allowing it to hold a piece of tissue paper: tarsal contact resulted in the cessation of flight. Flight could be reinitiated subsequently by removing the paper. The wind speed, strobe frequency, frame number and instantaneous vertical force were recorded simultaneously on a single video image for subsequent analysis of the flight quality. Each individual moth was flown until its vertical force production fell below about 75 % of body weight. After its final flight, the moth was immediately killed by chilling, and its mass measured.

(*d*) *Image analysis*

Negatives were scanned at 600 d.p.i. using a Kodak FilmScanner 2000, and the resulting electronic images were stored on Photo CD format disks. These images were opened in the Photoshop image-handling application on a Macintosh Quadra 650. The two images comprising each stereograph were first cropped and then aligned into their pair for viewing. Hard copies of these paired images were produced on a dye-sublimation printer at 300 d.p.i.

(*e*) *High-speed video recording of the wake dynamics*

A Kodak EktaPro 1000 high-speed video system, operating at 1000 frames per second, was used to record a side-view of the moth and its wake at an air speed of 1.8 m s^{-1}. The tethering set-up was the same as that for the still photography, but continuous illumination studio lamps replaced the strobe lighting. The moths were moved towards and away from the smoke to investigate the spanwise structure of the wake. The location of the smoke at any instant could be determined from a small top-view inset on the video image.

3. RESULTS

The fundamental wake elements which were observed will be illustrated for an airspeed of 1.8 m s^{-1}, where they were visualized most clearly. The effects on the wake structure of changing the air speed, or the radial position of the smoke, will then be considered. The sex and mass of the moths used in each analysed sequence are given in table 1 along with the measurements of mean vertical force generation, which were typically about 80 % of the body weight.

(*a*) *Elements of the wake structure*

Figure 2 shows stereophotographs illustrating the typical wake structure at various stages of a composite wingbeat for a female moth, ST20, at an airspeed of 1.8 m s^{-1} and with the smoke at 0.5*R*. The small metal sphere seen at the extreme right of each image lies in the plane of the undisturbed smoke and provides a marker against which the flow deviation perpendicular to the free-stream velocity can be gauged.

In figure 2*a* the wings are in the middle of the downstroke. Looking at the near field, the flow separates at the leading edge and reattaches to the upper surface in the posterior half of the wing. The enclosed leading-edge separation bubble is small, and was not always clearly visible. After reattaching to the upper surface, the air changes direction abruptly as it flows in a radial direction out towards the wingtip, where it rolls up into the tip vortex. The latter forms a vortex 'tube' running from the wingtip to the starting vortex which was formed during pronation. The tip vortex is clearest early in the downstroke when the smoke is intersecting the most distal quarter of the wing.

Downstream the structures formed during the preceding upstroke can be seen, lying much closer to the sagittal plane than the downstroke tube. The smoke streams have thinned and become closer, indicating that the air has higher velocity than in the

Table 1. *The experimental conditions and measured mean vertical force, as a percentage of body weight, for the flight sequences which are described in the text*

moth and sequence number	airspeed (m s^{-1})	smoke position (*R*)	mean vertical force (%)
effects of speed on wake structure			
ST20 female, mass 1.83 g			
I	0.4	0.5	74
II	1.8	0.5	79
III	3.7	0.5	85
IV	5.7	0.5	96
variation in wake structure with spanwise position			
ST24 male, mass 1.22 g			
I	1.8	0.25	—
II	1.8	0.50	74
III	1.8	0.75	70
IV	1.8	1.00	82
far wake structure ST3 male, mass 1.46 g			
I	0.8	0.5	79
II	1.8	0.5	82

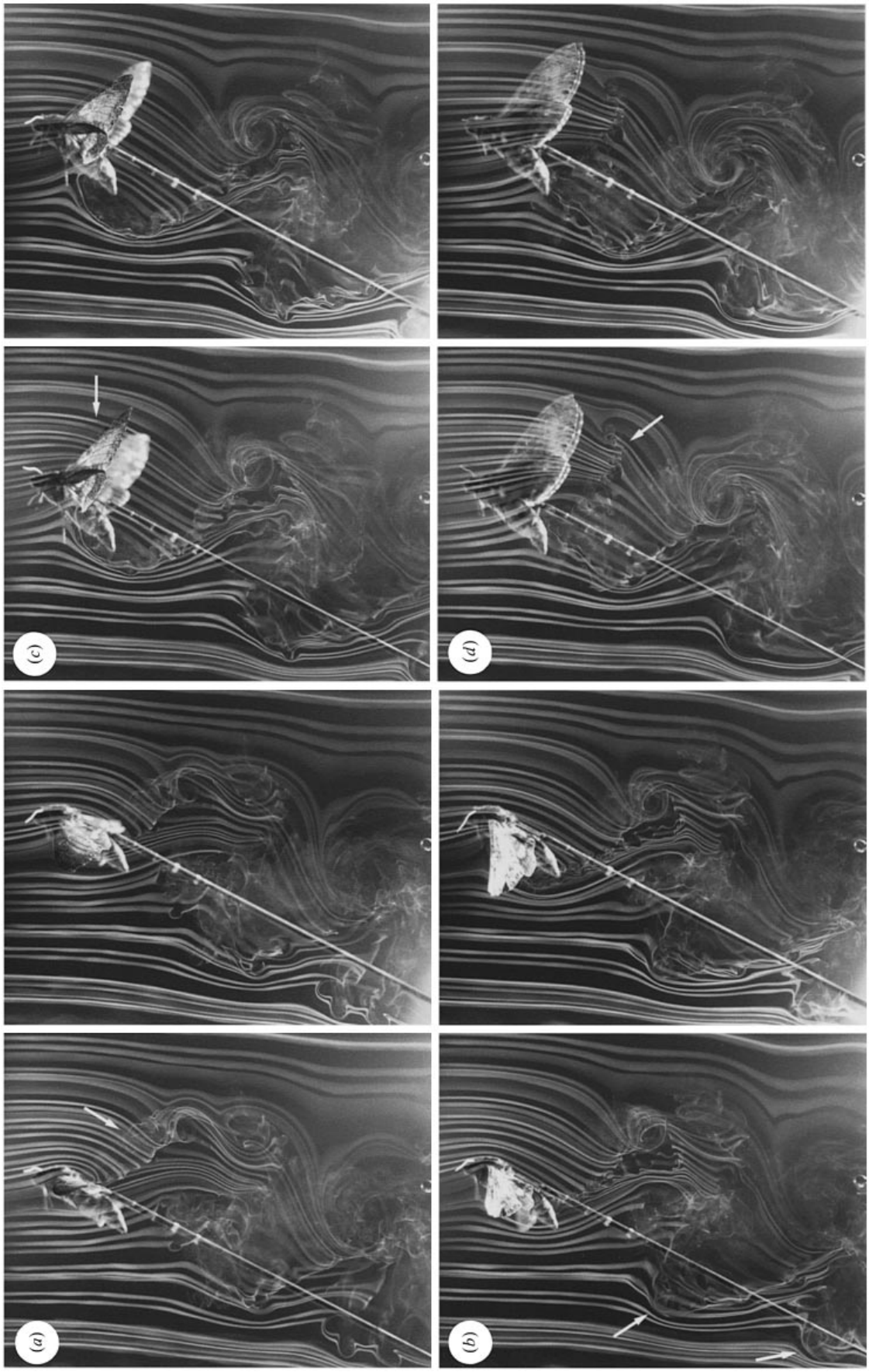

Figure 2. Stereophotographs showing the visualized wake at different stages in the wingbeat for moth ST20 at 1.8 m s^{-1}. The left and right photographs of each part correspond to the lower and upper camera views, respectively. In this stereo layout, the direction of the airflow is from the top to the bottom of the figure. (*a*) Mid-downstroke. The downstroke tip vortex is arrowed. (*b*) Supination. The supination vortices from the preceding two wingbeats are indicated. (*c*) Mid-upstroke. The influence of the bound circulation on the smoke streams is best seen by examining the offset of the arrowed stream across the wing. (*d*) Late upstroke. Tip vorticity (arrow) has been left in the wake. The smoke is at $0.5R$ throughout. The structures are explained further in the text.

downstroke vortex. In figure 2*b*, the upstroke structure has 'caught' that of the preceding downstroke, leading to complicated interactions between all the vortices.

Returning to the near field, the wings have reached the end of the downstroke and are in the middle of their supinatory rotation. The spanwise flow over the upper surface continued to the end of the translation, though its strength appears to decline towards the end of the half stroke, either as a result of wing deceleration or the smoke moving more inboard along the wing.

The transverse vorticity shed during supination should complete a 'downstroke vortex ring'. The details of vortex shedding are not clear in this sequence, and the result is a large, ill-defined area of vorticity. The corresponding vortices formed during the previous two supinations can also be identified and they show how the downstroke vortex rolls up into a wider vortex ring, with the vortex tube convecting slowly outwards and becoming larger in diameter as it does so. The downstream velocity of the vortex decreases with time: the spacing between the most recent vortex and the preceding one is greater than that between the latter and the earliest vortex. All three downstroke vortex rings are inclined at a small angle to the horizontal. In the near field, this results from the downward convection of the pronation and early downstroke tip vortices being slower than the downward component of the wingtip velocity. During subsequent roll-up of the vorticity, the vortex does not appear to become any more horizontal. The inclined path of the top streamlines underlines the influence of the induced velocity in imparting an overall downward momentum to the entire wake.

As supination proceeds, the area of vorticity increases in size as a transverse stopping vortex, and possibly some starting vorticity, is shed from the trailing edge. This region can be seen in figure 2*c*, where the wings have begun the upstroke translation. Where the leading edge has encountered the smoke trails being drawn down over the wings and body by the preceding downstroke vortex ring, it has cut cleanly through them at approximately a right angle. The smoke streams on either side of the wing are slightly offset, however, indicating a small amount of circulation around the wing.

Further downstream, as the wake continues to roll up, some of the upstroke flow has become almost transverse to the free-stream velocity, under the influence of the subsequent, and much more coherent, downstroke tip vortex. The smoke streams are running almost parallel to the camera axis immediately downstream of where this vortex can be seen in cross-section.

As the upstroke proceeds (figure 2*d*), the wings move rapidly backwards and, during the second half of the half stroke, in towards the body. The air below the wing follows, cutting through the air which had been drawn down between the dorsal wing surfaces by the preceding downstroke. At this boundary, tip vorticity can be seen. This vorticity is much weaker than its downstroke equivalent, but it is evidence of an increase in the circulation (and thus lift production) during the second half of the upstroke. The increase in force production appears to coincide with the change in the direction of the wing path. Transverse starting vorticity must have been left in the wake as the circulation grew, but its location cannot be identified in this frame.

Air is being accelerated in towards the body from both sides. The spanwise components cancel out and the net result is that the vertical upstroke vortex ring moves backwards along the sagittal plane. Downstream, the previous upstroke vortex is still essentially vertical, but its lower half is beginning to be being drawn downward with the downstroke wake.

Further details concerning many of the above features and the three-dimensional structure of the wake were obtained by comparing the images taken with the smoke at different radial positions for a male moth (ST24) also flying at 1.8 m s^{-1}. The leading-edge bubble appeared to grow in size along the length of the wing. With the smoke at 0.25*R* (figure 3*a*) there is no visible leading-edge bubble and the flow over the leading edge is smooth. The bubble can be seen at 0.5*R* (figure 3*b*) and it has enlarged further by 0.75*R* (figure 3*c*). The latter station is approximately where the vortex begins to break away from the wing surface and roll up with the tip vortex. A Karman vortex street shed from the near antenna can be seen above the body in figure 3*a*. No additional information was gained from the stereophotographs with the smoke at 1.0*R*.

Figure 4 provides more evidence that the upstroke is aerodynamically active. All three frames show the wings at a phase of the upstroke intermediate between figure 2*c* and 2*d*. Where the wingtips have passed through the smoke which had been dorsal to the wings, tip vorticity has been left in the wake (figure 4*b*, 4*c*). This vorticity is weaker at all spanwise stations than the downstroke equivalent, and the comparative narrowness of the upstroke jet indicates that the upstroke is only appreciably aerodynamically active during its second half. In the region of the supination vorticity there is the suggestion that there have been two distinct periods of shedding of transverse vorticity which were separated slightly in time and thus in location (figure 4*b*). The significance of this separation will be discussed later. Figure 4*a* shows most clearly the effects of the entrainment of the air upstream of the ventral surface of the wing; this air, along with any supination vorticity, follows the wing motion upwards and backwards during the upstroke translation.

(*b*) *Changes in the wake structure with flight speed*

As the flight speed of *M. sexta* changes so also do the relative magnitudes of the forward and induced velocities, and the wingbeat kinematics (Willmott 1995). The associated variation in the wake structure is illustrated in figures 5–7. The same moth (ST20) and smoke position (0.5*R*) were used for every speed.

Figure 5 shows stereophotographs of the wake at 0.4 m s^{-1}, a speed at which the ratio of forward velocity to flapping velocity falls below 0.1, placing it in the realm of 'hovering' flight as defined by Ellington (1984*a*). In comparison with the wake structure at 1.8 m s^{-1} (figure 2), the vortices from successive half strokes are less spread out in the direction of the

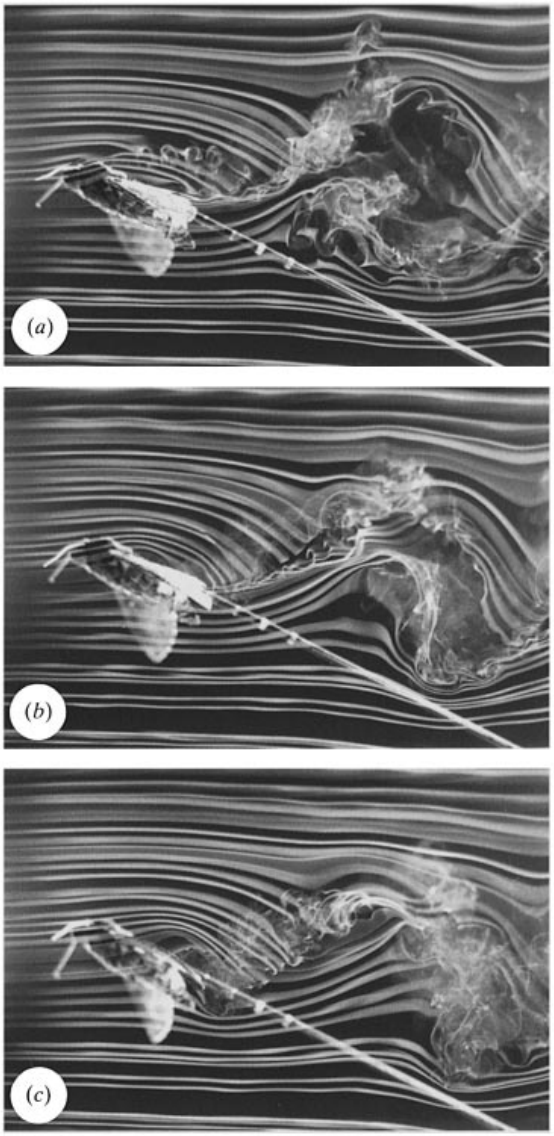

Figure 3. The changes in size of the leading-edge bubble with radial position. (*a*), (*b*) and (*c*) show the visualized mid-downstroke wake features with the smoke set at 0.25, 0.5 and 0.75 *R*, respectively. The moth is male ST24 and the airspeed is 1.8 m s^{-1}.

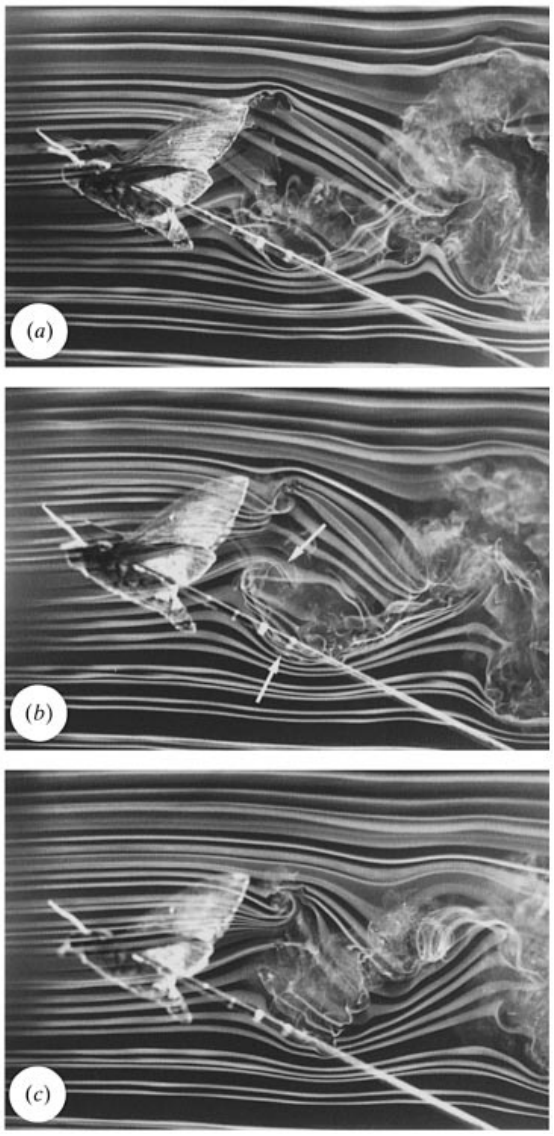

Figure 4. Evidence from the different radial smoke positions for an active upstroke. (*a*) The entrainment of the smoke below the moth is clearest with the smoke at 0.25 *R*. (*b*) Separation of the upstroke-starting vortex from the downstroke-stopping vortex is seen with the smoke at 0.5 *R*. The two periods of shedding of transverse vorticity are arrowed. By 0.75 *R* (*c*) the supination vortices are mixed up with the downstroke tip vortex, but the subsequent upstroke tip vortex can be seen. Experimental details as for figure 3.

free-stream velocity, leading to disruptive interference between them and to greater wake instability. The higher induced velocity at this lower flight speed also gives the whole wake a more pronounced vertical component to its motion.

These differences can be clearly seen in figure 5*a* with the wings in late downstroke. In the near field, there is clear evidence for the leading-edge separation, reattachment, and subsequent spanwise flow described for figure 2*a*. At the lower speed, however, the influence of the downstroke vortex is more evident: the streams above the body are being drawn down towards the vortex at a steeper angle and being accelerated through the centre of the vortex ring.

Any temporal separation between the stopping and starting vortex shedding during pronation does not result in significant spatial separation between these vortices because of the low airspeed. Instead, there is an ill-defined region of vorticity inboard of and slightly above the much more distinct tip vortex. The downstroke and upstroke paths are close together at stroke reversal and the close proximity of vortices, especially the tip vortices, has probably led to destructive instability both here and in the region of supination. The preceding upstroke vortex, which should be completed by a transverse stopping vortex shed during pronation, is moving close to the sagittal plane, having been drawn inwards more markedly than at 1.8 m s^{-1}. Very little remains of any earlier structures.

Figure 5*b* shows the wings in late supination, with an interesting leading-edge 'bubble' on the ventral surface of the wing. This bubble is consistent with a flex mechanism for the creation of circulation during isolated rotation. If this circulation remained attached

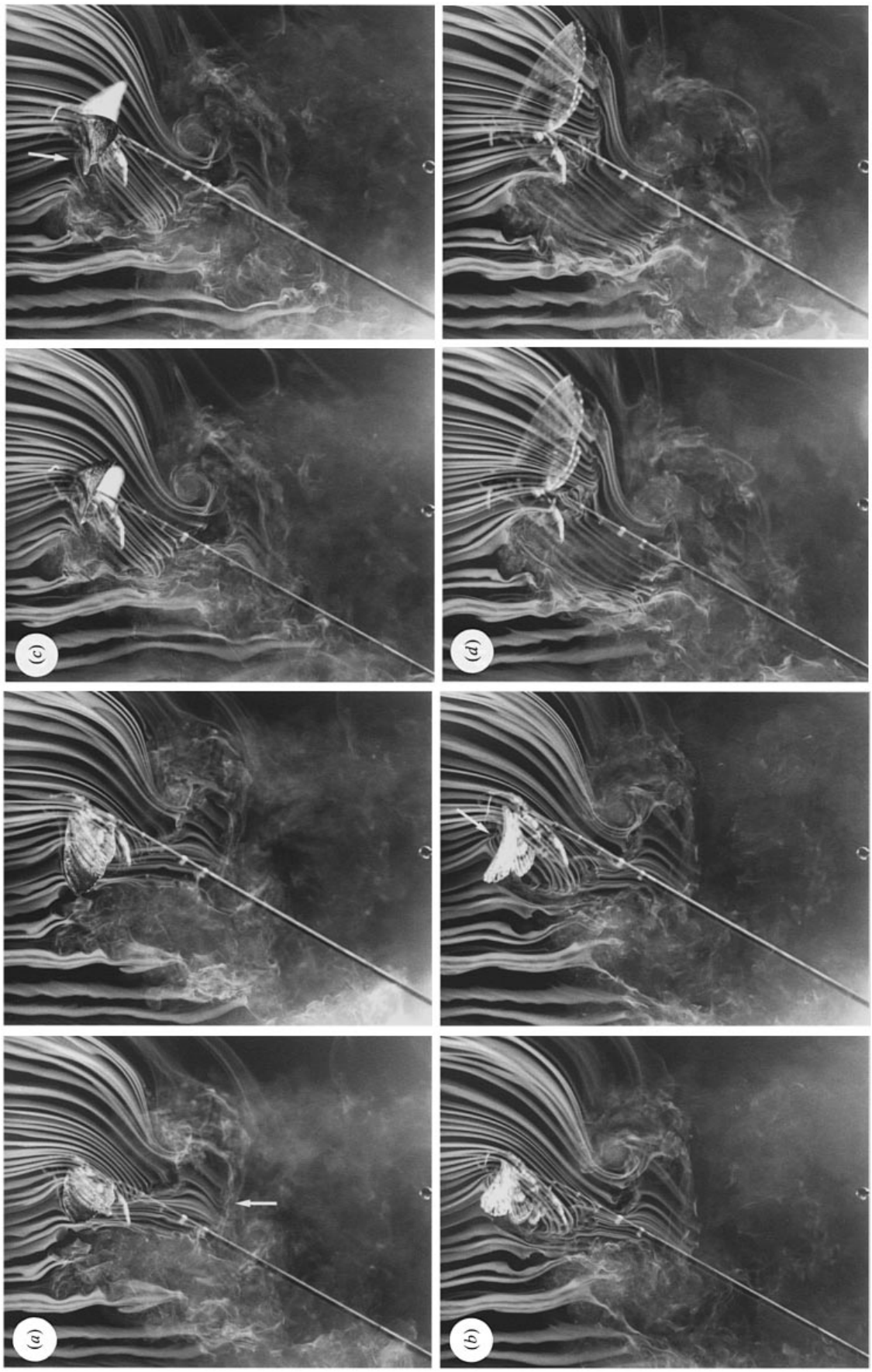

Figure 5. The influence on the wake of a decrease in the ratio of forward to induced velocity can be seen in stereophotographs for moth ST20 at 0.4 m s^{-1}. In comparison with the wake at 1.8 m s^{-1} (figure 2), (*a*) the entire wake is inclined at a greater angle to the horizontal and the compression of the distance between adjacent rings results in considerable destructive interference. By late downstroke the preceding upstroke features (arrow) are already becoming indistinct. (*b*) During supination, a combination of flexion and rotation leads to the shedding of leading-edge vorticity on the underside of the wing (arrow). (*c*) This vorticity is not recaptured at the start of the upstroke. Instead it is shed from the trailing edge (arrow). (*d*) The wing path during the late upstroke causes a pronounced movement of air in towards the sagittal plane. The smoke is at 0.5*R* throughout.

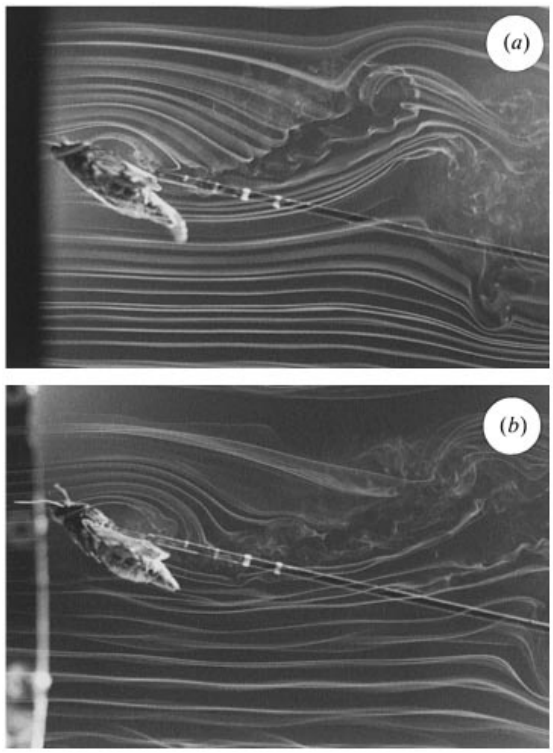

Figure 6. The leading-edge vortex increases in size with forward speed. For smoke at the same spanwise position ($0.5R$) the vortex is larger at 3.7 m s^{-1} (*a*) than it was at 1.8 m s^{-1} (figure 2*a*), and at 5.7 m s^{-1} (*b*) it nearly extends across the entire chord at this radial position. The underexposed strip at the left edge of (*a*) is the result of a slight asynchrony between the camera shutter and the strobe lighting.

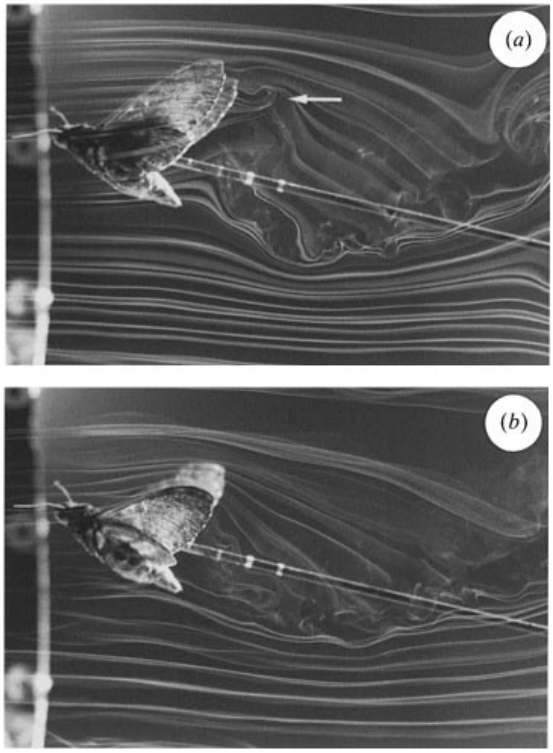

Figure 7. Upstroke features during fast forward flight. (*a*) At 3.7 m s^{-1} upstroke tip vorticity (arrow) can be seen downstream of the pronating wings. (*b*) At 5.7 m s^{-1} the smoke streams appear to be striking the morphological underside of the wing during the upstroke translation. There is no evidence of any transverse supination vorticity which might indicate a reversal of circulation between successive half strokes. The smoke is at $0.5R$.

to the wing, it would enhance lift production during the subsequent translation. At this speed, however, it is only a transient structure which is left behind as the upstroke translation begins (figure 5*c*).

The transverse vorticity shed during supination is better defined than in figure 2*c*, but its core still appears to have broken down. The wings are, once again, cutting cleanly through the smoke trails in early upstroke; this indicates the absence of any substantial lift production, and confirms that the leading-edge vortex created during rotation has not been recaptured. By figure 5*d*, the wings have passed through the smoke streams during the second half of the upstroke, generating similar tip vorticity to that seen in figure 2*d*. There is a pronounced inward movement of the air, reflecting the wing path late in the upstroke.

At forward speeds higher than 1.8 m s^{-1} the increasing diffuseness of the smoke and the streamwise stretching of the wake elements made the images harder to interpret unequivocally. A number of important observations were made, however. First, if the images from late-downstroke at 3.7 and 5.7 m s^{-1} (figure 6*a* and 6*b*, respectively) are compared with figure 2*b*, the leading-edge bubble can be seen to increase in size with forward velocity. By the highest speed, the bubble has grown until it almost stretches across the entire chord at the mid-span position.

The upstroke structures at the highest speeds are shown in figure 7. At 3.7 m s^{-1} (figure 7*a*) tip vorticity can be seen where the wing has cut through the smoke trails during the upstroke. The region of vorticity corresponding to the most recent supination again suggests that there were two distinct periods of shedding. At 5.7 m s^{-1} (figure 7*b*) there is a qualitative difference in the upstroke aerodynamics; the smoke trails are striking the morphological underside of the wing during the upstroke as well as the downstroke. This pattern indicates that the bound circulation has the same sense on the two half strokes and there would be no need for vorticity to be shed during the stroke reversal. Indeed, none of the frames recorded at this speed show any clear evidence that transverse vorticity has been shed during supination. The sense of rotation of the upstroke tip vortex must be the opposite of that seen at the lower speeds.

(*c*) *Far wake images*

Figure 8 shows wake images with a wider field of view at 0.8 and 1.8 m s^{-1}. The wake structure rapidly becomes disrupted as the vortex rings convect downstream. The only regular structure is the periodic drawing in of air around the positions of pronation and, for the higher speed only, supination. The wake axis is inclined at an angle of about 30° below the horizontal at 0.8 m s^{-1}, and about 10° at 1.8 m s^{-1}. The wake axis became more horizontal at even higher speeds, but the wake elements became so spread out that accurate estimates of the axis were not possible.

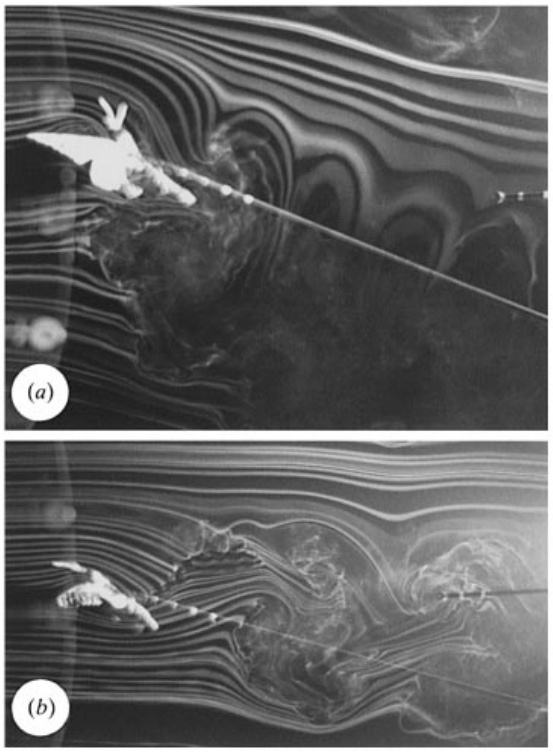

Figure 8. Wider angle views of the wake at (*a*) 0.8 and (*b*) 1.8 m s^{-1}. At the slower speed the detailed structure is rapidly lost and earlier vortex rings are indicated only by air drawn down into the region of pronation. At the higher speed the chain is coherent for longer but signs of breakdown, especially close to the supination vorticity, can be seen at the right side of the image.

(*d*) *High-speed video sequences*

Analysis of the high-speed video sequences was invaluable in helping to adjudicate between possible interpretations for several of the wake features described above. The very clear alternate shedding of vortex rings with each half stroke seen in the videos was, for example, unequivocal evidence for the presence of an aerodynamically active upstroke. The sequences also confirmed the sense of the circulation for some of the vortices, which could not be determined unambiguously from the still photographs.

4. DISCUSSION

(*a*) *The* M. sexta *wake structure*

The stereophotographs presented here provide the most detailed picture to date of the three-dimensional structure of the wake behind a flying insect. The general wake structure which they illustrate comprises a series of alternating horizontal and vertical vortex 'rings' which are generated by successive down- and upstrokes, respectively. This structure is presented in figure 9*a–d* which shows schematic representations of the streakline paths in late downstroke and late upstroke respectively, at 1.8 m s^{-1} (based on figure 2*b* and 2*d*). Regions of vorticity revealed by the streaklines are indicated by dashed lines. Solid arrows show the air flow, including the circulation around vortex tubes. During the downstroke, flow separation at the leading edge and reattachment over the posterior half of the upper surface lead to the formation of a small, but distinct, leading-edge vortex (LEV) whose size increases both from wingbase to wingtip, and over the course of the half stroke. The leading-edge vortex does not grow to the point at which it becomes unstable (as predicted from two-dimensional models) because a substantial spanwise flow transports the vorticity along the length of the wing and, ultimately, into a strong downstroke tip vortex (DTV). The strength of this radial flow can be seen from the sharp angle through which the air reattaching to the dorsal surface is turned toward the wingtip. The tip vorticity breaks away from the dorsal surface as a fairly broad vortex tube detaching from the final quarter of the wing length.

The tip vortices from the two wing couples are joined via transverse vorticity shed during pronation. Since there is no full clap in *Manduca*, separate transverse vorticity is shed by each wing (figure 10). It is not clear whether the stopping and starting vortices are shed together or whether they are formed independently and subsequently roll up into the diffuse region of pronation vorticity (PV) seen in the images. The transverse vortices on the two wing couples are close enough to cancel, especially in proximal regions, and merge into a single vortex. This vortex combines with the two tip vortices to form a 'U-shaped vortex tube' which is connected to the bound vorticity of the wing as described by Grodnitsky & Morozov (1992, 1993). At the end of the downstroke, the bound vorticity is shed as a downstroke-stopping vortex (DSV, figure 9*b*), which completes an approximately horizontal and not perfectly circular vortex 'ring'. The slight inclination of the ring to the horizontal gives a downwards and backwards impulse to the air and thus generates both weight support and thrust during the downstroke. The conventional circulation is augmented by the detached vortex lift derived from the leading-edge vorticity.

During supination, the leading-edge vortex moves rearward over the upper wing surface and is shed from the trailing edge. At the point when the leading edge starts to rotate, the wing couple flexes along a line close to the join between the fore- and hindwing. The higher velocity at the leading edge induces vortex shedding at the ventral surface, fitting the flex mechanism proposed by Ellington (1984*b*). The new leading-edge vortex is of the correct sense for enhancing the subsequent upstroke-bound circulation, if it remains attached to the wing. Surprisingly, perhaps, this does not happen at 0.4 m s^{-1}. The fate of this vorticity at higher speeds is not known.

At the start of the upstroke, there is only a weak circulation around the wings. This circulation grows as the translation proceeds, and an upstroke-starting vortex (USV), of the same sense as the downstroke-stopping vortex (DSV), is left behind in the wake (figure 9*b*). The temporal separation between the shedding of these two vortices is often visible as a distinct spatial separation. They are close enough to roll up into a single region of supination vorticity (SV, figure 9*d*), but the roll-up is unstable and yields a diffuse, broken-down core in the resultant vortex.

PHILOSOPHICAL TRANSACTIONS OF THE ROYAL SOCIETY B BIOLOGICAL SCIENCES

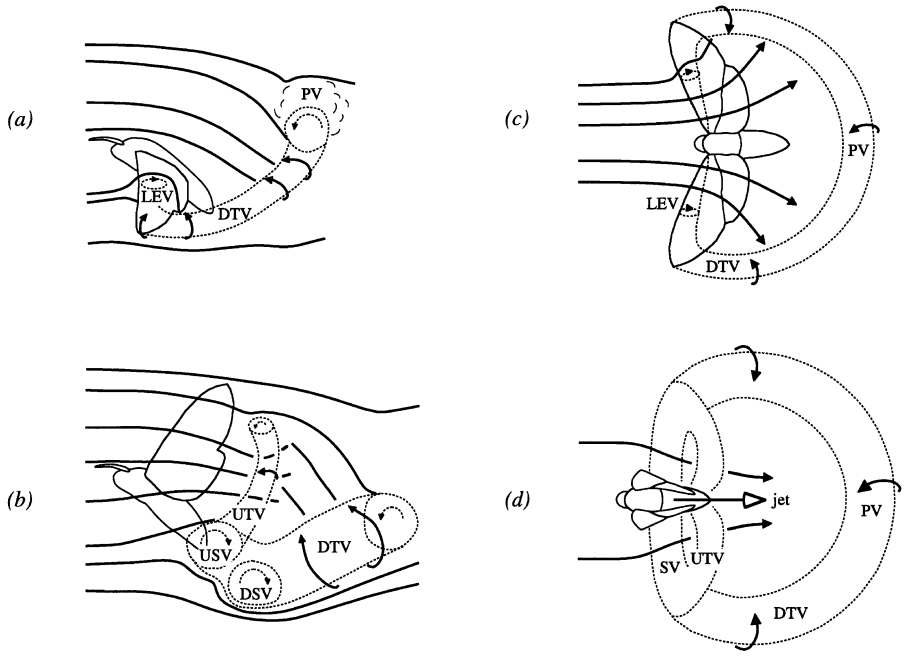

Figure 9. A generalized model for the wake structure. (*a*), (*b*) Schematic representations of the visualized wake features during late downstroke and late upstroke, respectively. The structures and their labels are explained further in the text. (*c*), (*d*) Dorsal views of the same features and of the accompanying air movements.

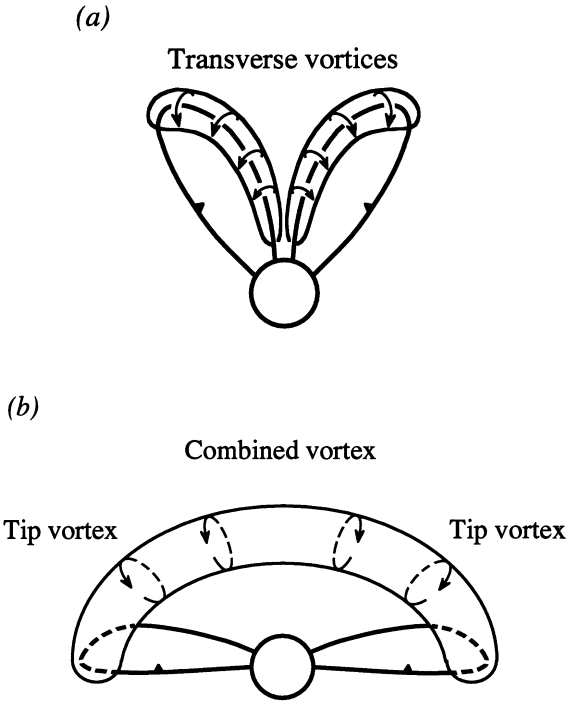

Figure 10. Formation of the 'upper U-shaped vortex' as envisaged by Grodnitsky & Morozov (1992, 1993). (*a*) Transverse vorticity is shed from the trailing edges of the two wing couples during pronation. These vortex tubes join proximally to form a combined vortex which is connected to the wings by the tip vortices. (*b*) As the downstroke proceeds, the shape of the combined vortex changes as it comes to form the central section of an inverted U-shaped vortex tube. Slightly modified from Ellington (1995), adapted from Grodnitsky & Morozov (1993).

The tip vorticity left in the wake where the tip has passed through the smoke streams provides confirmation that bound circulation is present during the upstroke. The upstroke tip vortex (UTV) becomes more intense as the half stroke proceeds, but it remains much weaker than its downstroke equivalent.

As the wings translate, the air below the ventral surface, including the supination vorticity, is drawn upwards, backwards and in towards the sagittal plane. The precise point at which the supination vortices from the two wing couples join and thus close the downstroke vortex ring is not certain, but it may not occur until their proximal ends have moved downstream towards or off the end of the abdomen. At the end of the upstroke, the transverse vorticity shed during pronation closes an approximately vertical upstroke vortex ring, which imparts horizontal momentum to the air. The reaction to this flow generates thrust during this phase of the wingbeat. During the majority of the upstroke, the air between the dorsal surfaces of the wings is drawn smoothly down over the body and wings by the downstroke vortex. The vertical vortex is instead comprised of air sucked in towards the sagittal plane from the two sides of the body. The spanwise components of these flows from the two sides of the body cancel out, leaving only the backwards component which provides thrust. The thrust is enhanced, late in pronation, by a small jet of air originating from the near clap and peel in the anojugal region. This jet was most clearly seen in the video sequences.

Dorsal views of the proposed vortex wake are given in figure 9*c* and 9*d*, showing the air motion on the downstroke and upstroke, respectively. The open-headed arrow in figure 9*d* shows the late upstroke jet originating from between the trailing edges of the hindwings. The regions of vorticity associated with stroke reversal are presented in their rolled-up forms (PV and SV), completing the vortex rings. For clarity, these regions are drawn as less diffuse than they appear in the stereo images.

A preliminary visualization study using a smaller but unnamed hawkmoth, which appears to be a member of the macroglossine genus *Hyles*, has been reported by Luttges (1989), who noted a strong tip vortex and a leading-edge vortex over the body. It is difficult to interpret these results, however, since the moth is clearly struggling to escape the tether, as acknowledged by the author: the body posture is unnatural, and 'very significant lateral forces' were generated.

The problems inherent in the interpretation of insect wake visualizations are evident in the very different models proposed by different authors. Brodsky (1994) reviewed his studies of a range of species and concluded that a separate vortex ring is shed at the end of each half stroke. In most instances adjacent vortices are linked through the vortices shed at stroke reversal, resulting in a chain of coupled vortex rings. The two major exceptions to this pattern were the peacock butterfly, *Inachis io*, for which the rings were separated by a full clap and fling during one or both stroke reversals (Brodsky 1991), and the crane fly, *Tipula paludosa*, which appeared to shed separate vortex rings on each side of the body, thus generating two parallel chains of coupled rings. Grodnitsky & Morozov (1993), however, investigated six functionally two-winged species, including the skipper, *Thymelicus lineola*, studied by Brodsky and a different *Tipula* species, and concluded that each wingbeat creates only a single vortex ring, which is generated during the downstroke and thrown off at supination. Such a wake would be similar to that characteristic for slow flight in birds and bats (Rayner 1995).

The results of the current study clearly show that for *M. sexta* vertical vortex rings are present in addition to the horizontal rings, though the wing is much less aerodynamically active during the upstroke than during the downstroke. In the near field, the formation of the upstroke vortex ring is not well visualized, even in the stereophotographs, but several observations confirm that this half stroke is aerodynamically active. The tip vorticity seen where the wing cuts through smoke streams is evidence of circulation. In addition, the transverse starting vortex shed during the early upstroke indicates that this circulation grows as the half stroke proceeds.

The hawkmoth wake structure is, therefore, similar to Brodsky's coupled vortex ring model and, in particular, to the 'slanted vortex street' variant noted for the skipper, *Thymelicus lineola* (Brodsky & Ivanov 1984; Brodsky & Grodnitsky 1985). This pattern, which results from the upstroke vortex ring being weaker than the downstroke equivalent, may be characteristic of medium-sized insects with a relatively low wingbeat frequency (Brodsky 1994). The *Manduca* wake structure is, however, clearly more complicated than Brodsky's model. The substantial three-dimensionality of the wake structure, as seen in the spanwise flow during the downstroke and the pronounced separation in the spanwise direction of the upstroke and downstroke vortex rings, has not been recorded before. These effects combine with the different convection velocities of the horizontal and vertical rings to give a complex coupling of the wake. The resultant wake structure becomes very intricate as close as only two or three wake elements downstream of the wings. The absence of an extended chain of well-defined vortex rings can be observed in figure 8.

(*b*) *Unsteady aerodynamic mechanisms in the near wake*

The essential features of the *Manduca* wake structure have, therefore, been determined. The stereophotographs have shown the location of the vortex rings and the influence they have on the air within the wake. This information, in combination with the video sequences, has enabled several unsteady mechanisms to be identified.

The most important observation in the near field was the near ubiquitous downstroke leading-edge vortex and, for the first time, the associated spanwise component of flow over the dorsal surface of the wing. Leading-edge vorticity has been observed before in the skipper (Brodsky & Grodnitsky 1985) and the peacock butterfly (Brodsky 1991), but this is the first study to provide good data on the size, shape and stability of the leading-edge separation bubble. The vortices are considerably smaller, but more stable, than those seen experimentally or predicted for two-dimensional models (e.g. Somps & Luttges 1985; Gustafson & Leben 1991; Dickinson & Götz 1993). Both observations can be explained by the spanwise flow, which transports vorticity out towards the wingtip before it can roll up and become unstable. The potential of such a flow for stabilizing the leading-edge vortex was first noted by Maxworthy (1979), but it has not previously been identified with real insects, possibly because of the use of light slices for visualization.

A leading-edge vortex stabilized by a radial flow component is a strong candidate for being an important lift-enhancing mechanism in many insect groups. The results for *M. sexta* suggest that the separation bubble would have been small in size at the low forward speeds used in previous visualization studies, which may explain why it was not observed. This possibility was acknowledged by Grodnitsky & Morozov (1993). Clear evidence for leading-edge vorticity in dragonflies has recently been obtained using a much finer resolution particle visualization technique by J. H. Weygandt (unpublished data).

The increase in size of the leading-edge bubble with forward speed may result from the increasing relative velocity of the wings and the greater number of chord lengths travelled during the downstroke. It was, however, slightly unexpected in light of the analyses of forward flight, which have concluded that the required contribution from unsteady aerodynamic mechanisms should decrease during fast forward flight (e.g. Dudley & DeVries 1990; Dudley & Ellington 1990; Willmott 1995). The strength of the leading-edge vortex is not, however, necessarily related to its size. Quantitative measurements of the strength both of this vortex and of the spanwise flow are now required.

The origins of these same two features are less certain. The leading-edge vortex could theoretically be

generated by the near clap and peel during pronation, or by a delayed stall mechanism during the downstroke translation. The evidence from this study for either a rotational or translational origin is equivocal. No leading-edge bubble was seen prior to translation, unlike *Inachis io* (Brodsky 1991), which performs a complete clap and peel. Similarly the wing spacing at the top of the stroke does not appear to be used to vary force generation. If the leading-edge vortex was formed during pronation then this distance could be used to modulate the downstroke force (Ellington 1995), but a kinematic analysis of *M. sexta* flight (Willmott 1995) showed that it is the position of supination rather than pronation which is varied with forward speed. Only during escape manoeuvres, and other extreme high-lift sequences, was a complete clap and peel approached. Under such situations the clap and peel may generate leading-edge vorticity during rotation, as in the peacock butterfly, but the efficacy of this mechanism during normal flight remains to be demonstrated.

A number of mechanisms could be contributing to the spanwise flow component. The spiral leading-edge vortex itself will induce an axial velocity component. Additionally, the process may be driven by the pressure gradient resulting from the velocity, and therefore pressure, gradient from the wingbase to the wingtip. Thirdly, the spanwise flow could result from 'centrifugal' acceleration. Once the air has reached the distal regions of the wing it will be drawn towards the wingtip by the tip vortex, as proposed by Brodsky (1991) and Grodnitsky & Morozov (1992). Further studies are required to distinguish between these possibilities.

The upstroke circulation appears to be translational in origin. Formation during supination of leading-edge vorticity of the correct sense to support a flex mechanism was observed for *Manduca* at 0.4 m s^{-1}, as it was for the skipper (Brodsky & Ivanov 1984), but the vorticity was not recaptured during the subsequent translation. It therefore cannot have enhanced the circulation or lift production. The limited disruption to the streaklines where the wing cuts through them early in the upstroke is further evidence that no substantial circulation has been retained from rotation. Instead, the circulation grows during the upstroke translation, as revealed by the shedding of a starting vortex which is separate from the downstroke stopping vortex. Delayed stall is the most likely candidate for lift enhancement during this phase. The relatively weak tip vortex shows, however, that the strength of the circulation does not approach that seen during the downstroke. The flow over the ventral surface is not easy to visualize against the wing, but there was no hint of a leading-edge vortex to enhance lift during the upstroke.

Identification of the pronation events is still inconclusive, as described above, but one mechanism could be seen in both the still and the video images. Late in the phase, as the posterior regions of the hindwings come together in a near or partial clap, they force out a jet of air from between their dorsal surfaces. This 'tunnel' mechanism for jet force generation was described by Bocharova-Messner & Aksyuk (1981), and has been subsequently recorded with the more extensive dorsal clap associated with feeding and migration flight in *I. io* (Brodsky 1991) and supported by a detailed study of wing movements during butterfly take-off (Brackenbury 1991). The efficiency of the mechanism is enhanced by the seal which is formed between the abdomen and the expanded anal lobes of the hindwing. The tunnel mechanism may contribute to lift and/or thrust generation, depending upon the body angle, wherever there is the required combination of a dorsal clap and expanded hindwings. It should be noted that Grodnitsky & Morozov (1993) were unable to verify this mechanism in their study of six functionally two-winged species, two of which exhibited a dorsal clap.

The remaining uncertainty about unsteady aerodynamic mechanisms reflects the difficulty in obtaining good visualization of the near field flow with real insects. The problem lies in delivering an adequate supply of visualization material into specific regions of interest. Ellington and Van den Berg therefore developed a complementary technique using model wings on which the point of smoke release can be controlled. Rather than releasing the marker into the flow upstream of the insect, it can instead be introduced directly into the air around the leading or trailing edge as required. The results for the near field flow during simulated hawkmoth hovering provide a more detailed insight into the leading-edge phenomena (Van den Berg & Ellington 1997*a*, *b*).

One final question which needs to be addressed is whether the same aerodynamic mechanisms can explain flight over the full range of speeds observed under natural conditions. A common pattern of vortex shedding has been recorded for *Manduca* over the range of speeds from 0.4 to 3.7 m s^{-1}, and this model may be appropriate for most functionally two-winged flight. However, plots of the wingtip paths relative to the surrounding air (Willmott 1995) suggest that the air strikes the ventral surface during the upstroke at fast forward speeds, and this has been confirmed by the smoke streams at 5.7 m s^{-1}. If the sense of the circulation remains the same during both half strokes then this will represent a very different flight regime, which will undoubtedly demand different aerodynamic solutions. The mean lift requirements are significantly lower at these speeds (Willmott 1995), and unsteady high-lift mechanisms would be expected to be less important here than at low speeds. No other data are available at present for insect flight at comparable speeds, and further detailed investigation of the mechanics of fast forward flight is needed.

The authors are very grateful to Mr Peter Goodyer and the EPSRC Instrument Pool for the loan of the Kodak EktaPro 1000 system. This work was supported by grants from the SERC, the BBSRC and the Hasselblad Foundation.

REFERENCES

Bocharova-Messner, O. M. & Aksyuk, T. S. 1981 Formation of a tunnel by wings of diurnal butterflies in flight (Lepidoptera, Rhopalocera). *Dokl. Akad. Nauk. SSSR* **260**, 1490–1493.

Brackenbury, J. H. 1991 Kinematics of take-off and climbing flight in butterflies. *J. Zool.* **224**, 251–270.

Brodsky, A. K. 1991 Vortex formation in the tethered flight of the peacock butterfly, *Inachis io* L. (Lepidoptera, Nymphalidae), and some aspects of insect flight evolution. *J. exp. Biol.* **161**, 77–95.

Brodsky, A. K. 1994 *The evolution of insect flight*. Oxford: Oxford University Press.

Brodsky, A. K. & Grodnitsky, D. L. 1985 Aerodynamics of tethered flight of skipper, *Thymelicus lineola* Ochs. (Lepidoptera, Hesperiidae). *Ent. Obozr.* **64**, 484–492.

Brodsky, A. K. & Ivanov, V. D. 1984 The role of vortices in insect flight. *Zool. Zhurn.* **63**, 197–208.

Campbell, J. F. 1976 Augmentation of vortex lift by spanwise blowing. *J. Aircraft* **13**, 727–732.

Cloupeau, M., Devillers, J. F. & Devezeaux, D. 1979 Direct measurements of instantaneous lift in desert locust; comparison with Jensen's experiments on detached wings. *J. exp. Biol.* **80**, 1–15.

Dickinson, M. H. 1994 The effects of wing rotation on unsteady aerodynamic performance at low Reynolds numbers. *J. exp. Biol.* **192**, 179–206.

Dickinson, M. H. & Götz, K. G. 1993 Unsteady aerodynamic performance of model wings at low Reynolds numbers. *J. exp. Biol.* **174**, 45–64.

Dudley, R. & DeVries, P. J. 1990 Flight physiology of migrating *Urania fulgens* (Uraniidae) moths: kinematics and aerodynamics of natural free flight. *J. Comp. Physiol.* A **167**, 145–154.

Dudley, R. & Ellington, C. P. 1990 Mechanics of forward flight in bumblebees. II. Quasi-steady lift and power requirements. *J. exp. Biol.* **148**, 53–88.

Ellington, C. P. 1980 Vortices and hovering flight. In *Instationäre Effekte an schwingenden Tierflügeln* (ed. W. Nachtigall), pp. 64–101. Wiesbaden: Franz Steiner.

Ellington, C. P. 1984*a* The aerodynamics of hovering insect flight. III. Kinematics. *Phil. Trans. R. Soc. Lond.* B **305**, 41–78.

Ellington, C. P. 1984*b* The aerodynamics of hovering insect flight. IV. Aerodynamic mechanisms. *Phil. Trans. R. Soc. Lond.* B **305**, 79–113.

Ellington, C. P. 1984*c* The aerodynamics of hovering insect flight. VI. Lift and power requirements. *Phil. Trans. R. Soc. Lond.* B **305**, 145–181.

Ellington, C. P. 1995 Unsteady aerodynamics of insect flight. In *Biological fluid dynamics* (ed. C. P. Ellington & T. J. Pedley), *Symp. Soc. exp. Biol.* **49**, 109–129.

Ennos, A. R. 1989 The kinematics and aerodynamics of the free flight of some Diptera. *J. exp. Biol.* **142**, 49–85.

Francis, R. H. & Cohen, J. 1933 The flow near a wing which starts suddenly from rest and then stalls. *Rep. Memo. aeronaut. Res. Comm.* (*Coun.*) no. 1561.

Grodnitsky, D. L. & Morozov, P. P. 1992 Flow visualization experiments on tethered flying green lacewings *Chrysopa dasyptera*. *J. exp. Biol.* **169**, 143–163.

Grodnitsky, D. L. & Morozov, P. P. 1993 Vortex formation during tethered flight of functionally and morphologically two-winged insects, including evolutionary considerations on insect flight. *J. exp. Biol.* **182**, 11–40.

Gursul, I. & Ho, C.-M. 1992 High aerodynamic loads on an airfoil submerged in an unsteady stream. *AIAA J.* **30**, 1117–1119.

Gustafson, K. & Leben, R. 1991 Computation of dragonfly aerodynamics. *Computer Physics Communications* **65**, 121–132.

Heinrich, B. 1970 Thoracic temperature stabilization by blood circulation in a free-flying moth. *Science, Wash.* **168**, 580–581.

Heinrich, B. 1971 Temperature regulation of the sphinx moth, *Manduca sexta*. II. Regulation of heat loss by control of blood circulation. *J. exp. Biol.* **54**, 153–166.

Jensen, M. 1956 Biology and physics of locust flight. III. The aerodynamics of locust flight. *Phil. Trans. R. Soc. Lond.* B **239**, 511–552.

Kramer, M. 1932 Die Zunahme des Maximalauftriebes von Tragflügeln bei plötzlicher Anstellwinkelvergrösserung (Böeneffekt). *Z. Flugtech. Motorluftschiff.* **23**, 185–189.

Luttges, M. W. 1989 Accomplished insect fliers. In *Frontiers in experimental fluid mechanics* (ed. M. Gad-el-Hak), lecture notes in engineering 46. Berlin: Springer.

Maxworthy, T. 1979 Experiments on the Weis-Fogh mechanism of lift generation by insects in hovering flight. Part 1. Dynamics of the 'fling'. *J. Fluid Mech.* **93**, 47–63.

Nachtigall, W. 1979 Rasche Richtungsänderungen und Torsionen schwingender Fliegenflügel und Hypothesen über zugeordnete instationäre Strömungseffekte. *J. Comp. Physiol.* **133**, 351–355.

Rayner, J. M. V. 1995 Dynamics of the vortex wakes of flying and swimming vertebrates. In *Biological fluid dynamics* (ed. C. P. Ellington & T. J. Pedley). *Symp. Soc. exp. Biol.* **49**, 131–155.

Somps, C. & Luttges, M. 1985 Dragonfly flight: novel uses of unsteady separated flows. *Science, Wash.* **228**, 1326–1329.

Spedding, G. R. 1992 The aerodynamics of flight. In *Mechanics of animal locomotion* (ed. R. McN. Alexander), *Adv. Comp. env. Physiol.* vol. 11, pp. 51–111. Berlin: Springer-Verlag.

Spedding, G. R. 1993 On the significance of unsteady effects in the aerodynamic performance of flying animals. *Contemp. Maths* **141**, 401–419.

Spedding, G. R., Rayner, J. M. V. & Pennycuick, C. J. 1984 Momentum and energy in the wake of a pigeon (*Columba livia*) in slow flight. *J. exp. Biol.* **111**, 81–102.

Sunada, S., Kawachi, K., Watanabe, I. & Azuma, A. 1993 Fundamental analysis of three-dimensional 'near fling'. *J. exp. Biol.* **183**, 217–248.

Van den Berg, C. & Ellington, C. P. 1997*a* The vortex wake of a 'hovering' model hawkmoth. *Phil. Trans. R. Soc. Lond.* B. **352**, 317–328.

Van den Berg, C. & Ellington, C. P. 1997*b* The three-dimensional leading-edge vortex of a 'hovering' model hawkmoth. *Phil. Trans. R. Soc. Lond.* B. **352**, 329–340.

Wakeling, J. M. 1995 Dragonfly aerodynamics. Ph.D. thesis. University of Cambridge.

Weis-Fogh, T. 1972 Energetics of hovering flight in hummingbirds and in *Drosophila*. *J. exp. Biol.* **56**, 79–104.

Weis-Fogh, T. 1973 Quick estimates of flight fitness in hovering animals, including novel mechanisms for lift production. *J. exp. Biol.* **59**, 169–230.

Wilkin, P. J. 1990 The instantaneous force on a desert locust, *Schistocerca gregaria* (Orthoptera: Acrididae), flying in a wind tunnel. *J. Kansas Ent. Soc.* **63**, 316–328.

Wilkin, P. J. & Williams, M. H. 1993 Comparison of the aerodynamic forces on a flying Sphingid moth with those predicted by quasi-steady theory. *Physiol. Zool.* **66**, 1015–1044.

Willmott, A. P. 1995 The mechanics of hawkmoth flight. Ph.D. thesis. University of Cambridge.

Wu, J. Z., Vakili, A. D. & Wu, J. M. 1991 Review of the physics of enhancing vortex lift by unsteady excitation. *Prog. Aerospace Sci.* **28**, 73–131.

Zanker, J. M. & Götz, K. G. 1990 The wing beat of *Drosophila Melanogaster*. II. Dynamics. *Phil. Trans. R. Soc. Lond.* B **327**, 19–44.

Received 9 May 1996; *accepted 22 August 1996*

PHILOSOPHICAL TRANSACTIONS OF THE ROYAL SOCIETY B BIOLOGICAL SCIENCES